ELSEVIER

Journal of Geometry and Physics 31 (1999) 75–95

JOURNAL OF GEOMETRY AND PHYSICS

Trapezoidal discrete surfaces: geometry and integrability

B.G. Konopelc199henko [a,*], W.K. Schief [b]

[a] *Dipartimento di Fisica, Università di Lecce, Via Arnesano, 73100 Lecce, Italy*

[b] *School of Mathematics, The University of New South Wales, Sydney, NSW 2052, Australia*

Received 12 October 1998

Abstract

Surfaces on which the lines of curvature form geodesics and parallels are discretized in a purely geometric manner. Discrete principal curvatures are defined and it is shown that the natural discrete Gauß equation is given by the standard discrete Schrödinger equation with the discrete Gaußian curvature as its potential. The subclass of discrete surfaces of revolution is considered and used to establish algebraic and geometric properties which are reminiscent of those known in the continuous case. Important connections with integrable discrete equations are also recorded.

Subj. Class.: Differential geometry
1991 MSC: 52CXX
Keywords: Discrete surfaces

1. Introduction

The study of coordinate systems which are canonical on a given class of surfaces constitutes an integral part of the differential geometry of surfaces. The most important coordinate systems to be found in the classical literature are asymptotic, conjugate, curvature and geodesics coordinates. In the past few years, the discretizations of asymptotic and conjugate coordinates proposed by Sauer [1,2] in the 1940s have been exploited to construct integrable discrete versions of pseudospherical surfaces [3], affine spheres [4,5] and conjugate coordinate systems [6–8]. Recently, lattices composed of cyclic quadrilaterals, which are relevant in computer aided surface design [9,10], have been identified as canonical discretizations of curvature coordinates. They have been used to obtain integrable discrete isothermic surfaces

* Corresponding author. Tel.: +10-39-832-320437; fax: +10-39-832-320505;
e-mail: konopel@lecce.infn.it

0393-0440/99/$ – see front matter
PII: S0393-0440(99)00010-8

[11], surfaces of constant positive Gaußian curvature [12], orthogonal coordinate systems [13–15] and coordinate systems of Egorov type [8]. However, it appears that geodesics and their corresponding orthogonal trajectories (parallels), which were introduced in Gauß' *Disquisitiones* [16], have not been considered in the context of integrable discrete geometry. The present paper addresses this issue.

As a first step towards the discretization of geodesic coordinates on surfaces, we here consider geodesics and parallels which constitute lines of curvature. We give natural discretizations of the geodesics and parallels and define discrete principal curvatures in a purely geometric manner. In the continuous case, the Gauß equation reduces to a Schrödinger equation with the Gaußian curvature as potential if one parametrizes a surface in terms of geodesic coordinates. Remarkably, it turns out that the canonical discrete analogue of the Gauß equation is given by the standard discrete Schrödinger equation with the product of the discrete principal curvatures being the potential. Hence, we here propose to define the discrete Gaußian curvature as the product of the discrete principal curvatures as in the continuous case.

Surfaces of revolution form a subclass of the surfaces considered here. Accordingly, we define discrete surfaces of revolution and discuss several specializations in order to test the validity of our definitions in the discrete case. Thus, we investigate in detail surfaces of constant Gaußian curvature, their Darboux transform and the class of Weingarten surfaces which is obtained by assuming that the principal curvatures are proportional. We establish important algebraic and geometric analogies between the discrete and continuous cases. In particular, connections with an integrable discrete pendulum equation, the integrable differential–difference Heisenberg spin equation [17,18] and a multi-parameter class of integrable mappings [19,20] are recorded.

2. Geodesic and parallel lines of curvature

This section is concerned with the properties of the class of surfaces on which the lines of curvature form geodesics and their associated orthogonal trajectories. We give canonical examples of such surfaces which will be used to 'test' the discretization procedure discussed in the next section.

2.1. *Principle curvatures and the Gauß equation*

If a surface $\Sigma: \boldsymbol{r} = \boldsymbol{r}(s,t)$ in Euclidean space $\mathbb{R}^3$ is parametrized in terms of geodesic coordinates, that is a family of geodesics and their orthogonal trajectories (parallels), then the first fundamental form $\mathrm{I} = \mathrm{d}\boldsymbol{r} \cdot \mathrm{d}\boldsymbol{r}$ takes the simple form

$$\mathrm{I} = \mathrm{d}s^2 + \phi^2 \, \mathrm{d}t^2. \tag{2.1}$$

Here, the geodesics $t = \text{const.}$ are parametrized in terms of arclength, that is $\boldsymbol{r}_s^2 = 1$, and the lines $s = \text{const.}$ form a family of parallels on the surface. According to the *Theorema egregium* [21], the Gaußian curvature of the surface may be expressed entirely in terms of the

coefficients of the first fundamental form. In particular, in the present case, the Gauß equation takes the form of a Schrödinger equation with the Gaußian curvature $\mathcal{K}$ as potential [21]:

$$\phi_{ss} + \mathcal{K}\phi = 0. \tag{2.2}$$

In the sequel, we focus on the subclass of surfaces for which the geodesics and parallels constitute lines of curvature. In this case, the second fundamental form $\mathrm{II} = -\mathrm{d}\boldsymbol{N} \cdot \mathrm{d}\boldsymbol{r}$ is purely diagonal, viz.

$$\mathrm{II} = \kappa^{(s)}\,\mathrm{d}s^2 + \kappa^{(t)}\phi^2\,\mathrm{d}t^2, \tag{2.3}$$

where $\boldsymbol{N}$ is the unit normal to the surface and $\kappa^{(s)}$, $\kappa^{(t)}$ denote the principal curvatures of the s- and t-curvature lines, respectively. The Gaußian curvature is then given by

$$\mathcal{K} = \kappa^{(s)}\kappa^{(t)}. \tag{2.4}$$

The principal curvatures may be conveniently characterized in terms of properties of the geodesics. Thus, the unit tangent $\boldsymbol{t}$, principal normal $\boldsymbol{n}$ and binormal $\boldsymbol{b}$ attached to the s-lines satisfy the linear Serret–Frenet equations [21]:

$$\begin{pmatrix} \boldsymbol{t} \\ \boldsymbol{n} \\ \boldsymbol{b} \end{pmatrix}_s = \begin{pmatrix} 0 & \kappa & 0 \\ -\kappa & 0 & \tau \\ 0 & -\tau & 0 \end{pmatrix} \begin{pmatrix} \boldsymbol{t} \\ \boldsymbol{n} \\ \boldsymbol{b} \end{pmatrix}, \tag{2.5}$$

with κ and τ being the corresponding curvature and torsion. Consequently, the right-handed orthonormal triad $(\boldsymbol{t}, \boldsymbol{n}, \boldsymbol{b})$ forms a canonical frame on the surface Σ since

$$\boldsymbol{r}_s = \boldsymbol{t}, \tag{2.6a}$$

$$\boldsymbol{r}_t = \phi\boldsymbol{b}, \tag{2.6b}$$

$$\boldsymbol{N} = \boldsymbol{n} \tag{2.6c}$$

and the principal curvatures read

$$\kappa^{(s)} = \kappa, \tag{2.7a}$$

$$\kappa^{(t)} = -\frac{\boldsymbol{b} \cdot \boldsymbol{n}_t}{\phi}. \tag{2.7b}$$

For convenience, the surface and principal normals have been chosen to have the same orientation.

In Section 3, it is shown that the above relations for the principal curvatures admit canonical discrete counterparts which may be obtained in a purely geometric manner.

2.2. *Surfaces of revolution*

An important subclass of the surfaces considered here are surfaces of revolution. A surface of revolution is generated by a planar curve (generator) which is rotated around an axis lying in the plane of the generator. The meridians of the surface of revolution are the geodesics

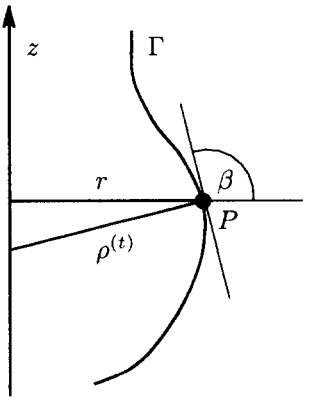

Fig. 1. The generator of a surface of revolution.

t = const. and the parallels s = const. consist of circles. Without loss of generality, the position vector $\boldsymbol{r} = \boldsymbol{r}(s, t)$ may be taken to be

$$\boldsymbol{r} = \begin{pmatrix} r(s)\cos(\omega t) \\ r(s)\sin(\omega t) \\ z(s) \end{pmatrix}, \tag{2.8}$$

where the functions $r(s)$ and $z(s)$ are related by the arclength condition

$$r_s^2 + z_s^2 = 1. \tag{2.9}$$

In order to be able to compare the continuous case with the discrete one, the constant angular velocity ω has not been scaled to unity. The curve $\Gamma: \boldsymbol{r} = \boldsymbol{r}(s, 0)$ constitutes the generator of the surface of revolution. The constraint (2.9) may be solved identically by introducing an angle $\beta(s)$ according to

$$r_s = \cos\beta, \tag{2.10a}$$

$$z_s = \sin\beta. \tag{2.10b}$$

The geometric relation between r, z and β is illustrated in Fig. 1.

The principal curvatures are readily derived from the representation (2.10). They are given by

$$\kappa^{(s)} = \beta_s, \quad \kappa^{(t)} = \frac{\sin\beta}{r}. \tag{2.11}$$

In view of a canonical discretization procedure, it turns out convenient to be to focus on the standard geometric interpretation of the principal curvatures in this case. Thus, given a point P on the surface of revolution, the osculating circle associated with the meridian passing through P lies in the plane spanned by the axis of rotation and the meridian. If we denote its radius by ρ, the principal curvature $\kappa^{(s)}$ takes the form

$$\kappa^{(s)} = \kappa = \frac{1}{\rho}. \tag{2.12}$$

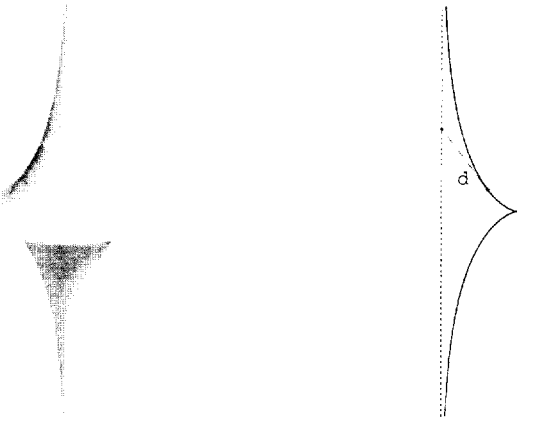

Fig. 2. The pseudopshere and its generator (tractrix).

On the other hand, it is readily verified that

$$\kappa^{(t)} = \frac{1}{\rho^{(t)}}, \tag{2.13}$$

where $\rho^{(t)}$ is the distance between the point P and the axis in the direction of the (principal) normal (cf. Fig. 1). It is also noted that the Gauß equation (2.2) may be regarded as a Schrödinger equation for the radial distance r since $\phi = \omega r$ and whence

$$r_{ss} + \mathcal{K} r = 0. \tag{2.14}$$

2.2.1. The pseudosphere

In the case of pseudospherical surfaces, that is without loss of generality, $\mathcal{K} = -1$, the Schrödinger equation (2.14) admits the first-order reduction

$$r_s = \pm r. \tag{2.15}$$

This implies that the distance of a point on the generator to the axis in tangential direction is

$$d = \left| \frac{r}{\cos\beta} \right| = \left| \frac{r}{r_s} \right| = 1 = \text{const.} \tag{2.16}$$

The latter property defines the classical *tractrix* which is displayed in Fig. 2. The associated surface of revolution constitutes the *pseudosphere*.

2.2.2. A Hasimoto surface of revolution

The classical Darboux transformation [22] provides a purely algebraic means of generating a sequence of potentials in a Schrödinger equation along with their corresponding eigenfunctions if the eigenfunctions associated with a seed potential are known. It is therefore natural to investigate the action of the Darboux transformation on (2.14). Here, we

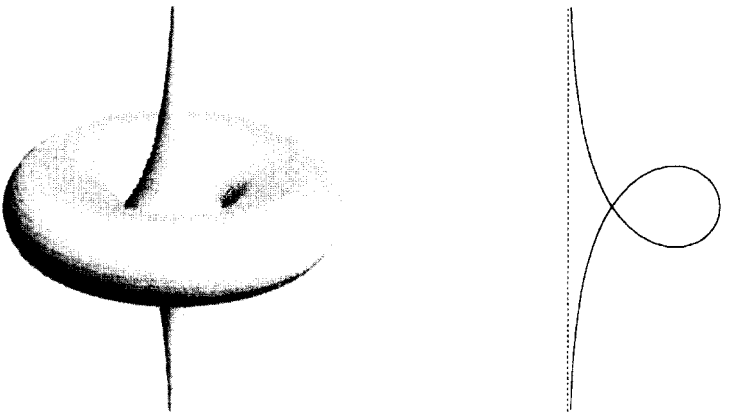

Fig. 3. A Hasimoto surface of revolution and its generator.

consider a degenerate Darboux transformation which reads as follows: if r and $\hat{r}$ are two solutions of the Schrödinger equation (2.14) with seed potential $\mathcal{K}$, then another solution of the Schrödinger equation is given by

$$r' = \hat{r}_s - \frac{r_s}{r}\hat{r}, \quad \mathcal{K}' = \mathcal{K} - 2(\ln r)_{ss}. \tag{2.17}$$

However, since the Wronskian $w(r, \hat{r}) = r\hat{r}_s - r_s\hat{r}$ is constant, the above transformation for r reduces to an 'inversion'

$$r' = \frac{c}{r}, \tag{2.18}$$

where c is an arbitrary constant.

Once again, it is instructive to consider the simplest case $\mathcal{K} = -1$. Hence,

$$r = \cosh s, \quad r' = \frac{2}{\cosh s} \tag{2.19}$$

form a corresponding pair of eigenfunctions with an associated new potential

$$\mathcal{K}' = -1 - \frac{1}{\cosh^2 s} \tag{2.20}$$

and integration of the primed version of the relations (2.10b) yields

$$z' = -s + 2\tanh s \tag{2.21}$$

without loss of generality. The corresponding generator Γ' is depicted in Fig. 3. It contains a loop and therefore generates a self-intersecting surface of revolution.

The appearance of a one-soliton sech^2-potential and a 'loop soliton' as generator is not coincidental. Indeed, the connection with soliton theory is readily established if one makes use of the fact that the new principal curvature $\kappa^{(s)\prime}$ reads

$$\kappa^{(s)\prime} = \kappa' = \beta_s' = r'. \tag{2.22}$$

Thus, on the one hand, it is natural to consider the general case of a surface of revolution subject to the constraint

$$r = \tilde{c}\kappa = \tilde{c}\beta_s, \tag{2.23}$$

where $\tilde{c}$ is an arbitrary constant. Insertion of this condition into (2.10a) produces the pendulum equation

$$\tilde{c}\beta_{ss} = \cos\beta. \tag{2.24}$$

It turns out that the well-known kink solution of the pendulum equation gives rise to the above surface of revolution.

On the other hand, combination of (2.22) and the primed version of (2.6b) shows that $\boldsymbol{r}'_t = \omega\kappa'\boldsymbol{b}'$ which implies that the generator Γ' evolves in binormal direction with speed proportional to the curvature κ'. This kind of evolution of a curve has been discussed by Hasimoto [23] in connection with the self-induced motion of a thin isolated vortex filament travelling without stretching in an incompressible fluid. Thus, if $\boldsymbol{r}(s,t)$ denotes the position of the vortex filament in space, then its motion may be shown to be constrained by

$$\boldsymbol{r}_t = \kappa\boldsymbol{b}, \tag{2.25a}$$

$$\boldsymbol{r}_s^2 = 1. \tag{2.25b}$$

The latter condition encodes the assumption of a nonstretching curve (filament). Since the binormal $\boldsymbol{b}$ is orthogonal to both the unit tangent $\boldsymbol{t} = \boldsymbol{r}_s$ and the principal normal $\boldsymbol{n}$, the Serret–Frenet equations (2.5) deliver

$$\kappa\boldsymbol{b} = \boldsymbol{t} \times \boldsymbol{t}_s. \tag{2.26}$$

Consequently, cross-differentiation of (2.25a) and $\boldsymbol{r}_s = \boldsymbol{t}$ results in the integrable Heisenberg spin equation

$$\boldsymbol{t}_t = \boldsymbol{t} \times \boldsymbol{t}_{ss}. \tag{2.27}$$

The latter is linked to the nonlinear Schrödinger (NLS) equation via a gauge (Miura-type) transformation [24,25] and may also be mapped to a complex loop soliton equation by employing a reciprocal transformation. The stationary one-soliton solution of the NLS equation induces a motion of the filament in such a way that the above surface of revolution is swept out. Moreover, the corresponding solution of the loop soliton equation at any fixed time t is represented by the generator of that surface [26].

2.2.3. *Weingarten surfaces*

A class of surfaces which contains surfaces of constant Gaußian curvature, constant mean curvature and minimal surfaces was first studied by Weingarten [21] in the last century. Weingarten surfaces are defined by the property that the principal curvatures be functionally dependent. Surfaces of revolution constitute a subclass of Weingarten surfaces since the principal curvatures depend only on the arclength parameter s and hence $\kappa^{(t)} = F(\kappa^{(s)})$ in

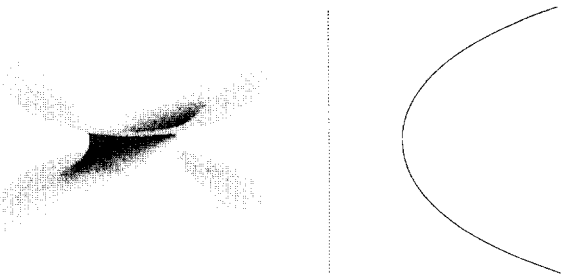

Fig. 4. The catenoid and its generator (catenary).

the generic case. Here, we briefly mention (Weingarten) surfaces of revolution for which a relation of the form

$$\kappa^{(s)} = c\kappa^{(t)}, \quad c = \text{const.} \tag{2.28}$$

holds. In the case $c = 1$, it is readily shown that the principal curvatures are constant and the meridians are circles. Hence, the corresponding surfaces of revolution constitute spheres. On the other hand, if the surface is minimal, that is

$$\mathcal{H} = \kappa^{(s)} + \kappa^{(t)} = 0, \tag{2.29}$$

then the classical *catenoid* is obtained (Fig. 4).

It is natural to enquire as to whether there exists some intersection between the classes (2.23) and (2.28). Thus, insertion of r as given by (2.23) into the constraint (2.28) produces the relation

$$\tilde{c}\beta_s^2 - c\sin\beta = I = 0. \tag{2.30}$$

Differentiation shows that I is a first integral of the pendulum equation (2.24) if and only if $c = 2$. Since $\tilde{c}$ is arbitrary, the complete class of surfaces of revolution with

$$\kappa^{(s)} = 2\kappa^{(t)} \tag{2.31}$$

is therefore contained in the 'Hasimoto' class (2.23). The discrete analogue of this result is presented in Section 3.2.3.

3. Trapezoidal quadrilateral lattices

Here, we are concerned with a canonical discretization of the surfaces discussed in the previous section. More precisely, coordinate systems which consist of geodesic and parallel lines of curvature are discretized. To this end, it is assumed that 'discrete coordinate lines' constitute coordinate polygons $\boldsymbol{r} = \boldsymbol{r}(n_i = \text{const.})$, $i = 1, 2$ on a $\mathbb{Z}^2$ lattice

$$\boldsymbol{r} : \mathbb{Z}^2 \to \mathbb{R}^3, \quad (n_1, n_2) \mapsto \boldsymbol{r}(n_1, n_2). \tag{3.1}$$

In the sequel, the arguments of any vertex $\boldsymbol{r} = \boldsymbol{r}(n_1, n_2)$ will be suppressed and its four neighbours denoted by

$$\begin{aligned} &\boldsymbol{r}_1 = \boldsymbol{r}(n_1 + 1, n_2), \quad \boldsymbol{r}_2 = \boldsymbol{r}(n_1, n_2 + 1), \\ &\boldsymbol{r}_{\bar{1}} = \boldsymbol{r}(n_1 - 1, n_2), \quad \boldsymbol{r}_{\bar{2}} = \boldsymbol{r}(n_1, n_2 - 1). \end{aligned} \tag{3.2}$$

Other vertices are represented by multiple indices. For instance, $(\boldsymbol{r}, \boldsymbol{r}_1, \boldsymbol{r}_2, \boldsymbol{r}_{12})$ designates an elementary quadrilateral.

As mentioned in Section 1, two-dimensional cyclic quadrilateral lattices which are such that the vertices of any elementary quadrilateral lie on a circle have proven to be the appropriate discrete analogue of surfaces parametrized in terms of lines of curvature in the context of integrable discretizations of particular classes of surfaces such as isothermic surfaces [11] or coordinate surfaces of multi-dimensional orthogonal coordinate systems [13–15]. On the other hand, polygons with equidistant vertices have been successfully used as discretizations of curves parametrized in terms of arclength [3,27]. Now, the fundamental forms (2.1) and (2.3) show that the class of surfaces discussed in Section 2 may be equivalently characterized by the existence of a family of lines of curvature which admits a parametrization in terms of arclength. Thus, it is natural to consider the class of 'discrete surfaces' which have the following properties:

(i) *Circularity.* The elementary quadrilaterals $(\boldsymbol{r}, \boldsymbol{r}_1, \boldsymbol{r}_2, \boldsymbol{r}_{12})$ are inscribed in circles.

(ii) *Discrete arclength parametrization.* The vertices of the coordinate polygons $\boldsymbol{r} = \boldsymbol{r}(n_2 = \text{const.})$ are equidistant and the distance does not depend on n_2, that is

$$|\boldsymbol{r}_1 - \boldsymbol{r}| = 1 \tag{3.3}$$

without loss of generality.

This implies that the elementary quadrilaterals constitute isosceles trapezoids with 'vertical' sides being of unit length. For brevity, we refer to the above class of lattices as *trapezoidal quadrilateral lattices* or *trapezoidal discrete surfaces*. It is noted that corresponding edges of the coordinate polygons $\boldsymbol{r} = \boldsymbol{r}(n_1 = \text{constant})$ are parallel, that is

$$\boldsymbol{r}_2 - \boldsymbol{r} \parallel \boldsymbol{r}_{12} - \boldsymbol{r}_1. \tag{3.4}$$

Hence, the n_1-coordinate polygons may be regarded as discrete geodesics while the n_2-coordinate polygons form a family of parallel polygons in complete analogy with the notion of geodesic parallels in the continuous case.

3.1. Discrete principle curvatures and a discrete Gauß equation

In order to construct a discrete counterpart of the Gauß equation (2.2), it is necessary to give natural geometric analogues of the principal curvatures $\kappa^{(s)}$ and $\kappa^{(t)}$. For this purpose, we first recall the standard definition of the radius of curvature for a curve in space. Consider a point P on a curve and two sufficiently close points P_1 and P_2 on this curve on either side of P. The circle passing through these three points is uniquely defined and the limiting circle as $P_1, P_2 \to P$ is called the osculating circle of the curve at P. Its radius ρ is termed the radius of curvature at P and $\kappa = 1/\rho$ is the corresponding curvature.

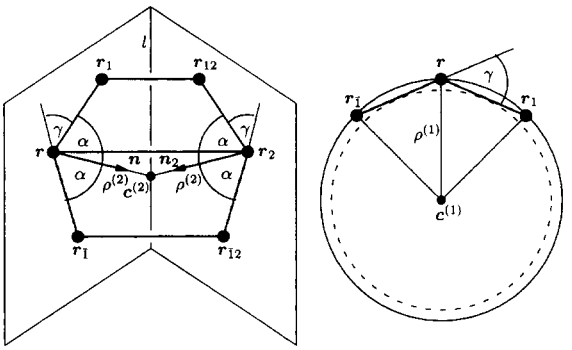

Fig. 5. The definition of the discrete principal curvatures.

In the case of the arclength parametrized discrete geodesics, we define the circle passing through three adjacent vertices $\boldsymbol{r}_{\bar{1}}, \boldsymbol{r}$ and $\boldsymbol{r}_1$ as the osculating circle at $\boldsymbol{r}$. [1] We regard the radius ρ of the osculating circle as the radius of curvature and its inverse $\kappa = 1/\rho$ as the curvature of the geodesic at $\boldsymbol{r}$. In analogy with the continuous case, we therefore define the discrete principal curvature $\kappa^{(1)}$ associated with the discrete geodesic by

$$\kappa^{(1)} = \kappa = \frac{1}{\rho} \tag{3.5}$$

and make the identification $\rho^{(1)} = \rho$. In terms of the angle between two adjacent edges, this means that

$$\kappa^{(1)} = 2\sin\frac{\gamma}{2}, \quad \cos\gamma = (\boldsymbol{r}_1 - \boldsymbol{r}) \cdot (\boldsymbol{r} - \boldsymbol{r}_{\bar{1}}) \tag{3.6}$$

as indicated in Fig. 5.

It is interesting to note that the centre of the osculating circle may also be constructed by means of an analogue of a classical method given by Nikolaides [28]. Thus, consider a planar curve $\Gamma: \boldsymbol{r} = \boldsymbol{r}(s)$ parametrized in terms of arclength for convenience. Given a point P on the curve with position vector $\boldsymbol{r}$, we denote by P^* the point which has the distance d from P in tangential direction, where d is an arbitrary constant. As P moves along the curve Γ, the point P^* sweeps out a curve Γ^* with parametrization

$$\boldsymbol{r}^* = \boldsymbol{r} + d\frac{\mathrm{d}\boldsymbol{r}}{\mathrm{d}s}. \tag{3.7}$$

One may then show that the principal normals $\boldsymbol{n}$ and $\boldsymbol{n}^*$ at corresponding points P and P^* meet at the centre of the osculating circle associated with P. In the discrete case, we consider a polygon $\Gamma: \boldsymbol{r} = \boldsymbol{r}(n_1)$ subject to the discrete arclength condition $|\boldsymbol{r}_1 - \boldsymbol{r}| = 1$. The edges of Γ may be mapped to the vertices of a polygon Γ^* according to

$$\boldsymbol{r}^* = \boldsymbol{r} + d(\boldsymbol{r}_1 - \boldsymbol{r}), \quad d = \text{const.} \tag{3.8}$$

[1] We usually commit the impropriety of referring to $\boldsymbol{r}$ as a vertex even though, strictly speaking, $\boldsymbol{r}$ is the position vector associated with a vertex.

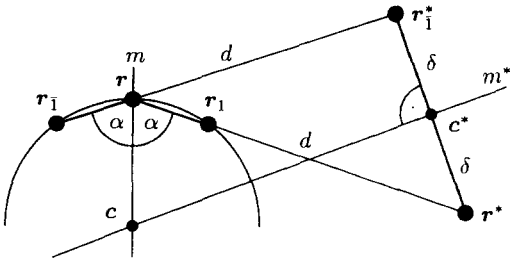

Fig. 6. Construction of the center of the osculating circle à la Nikolaides.

so that $r^* - r$ is 'tangent' to Γ and the distance $|r^* - r| = d$ is constant. By construction, the vertices $r_{\bar{1}}, r, r_1, r_{\bar{1}}^*, r^*$ and c lie on a plane as illustrated in Fig. 6. In fact, it is readily verified that the perpendicular bisector m^* of the edge $r^* - r_{\bar{1}}^*$ and the bisector m of $(r_{\bar{1}}, r, r_1)$ intersect at the centre c of the osculating circle associated with r. Hence, as in the continuous case, the lines m and m^* which are 'normal' to the polygons Γ and Γ^* respectively meet at the centre of the corresponding osculating circle.

The principal curvature associated with the discrete parallels is readily defined if one investigates the properties of two neighbouring trapezoids $(r, r_{\bar{1}}, r_2, r_{\bar{1}2})$ and (r, r_1, r_2, r_{12}) (cf. Fig. 5). Thus, the polygons $(r_{\bar{1}}, r, r_1)$ and $(r_{\bar{1}2}, r_2, r_{12})$ define two planes which intersect at a straight line l. This line may be regarded as a 'local axis of revolution' as the polygon $(r_{\bar{1}2}, r_2, r_{12})$ is obtained from the polygon $(r_{\bar{1}}, r, r_1)$ by rotation around l. In this way, the vertex r sweeps out an arc of a circle which may be interpreted as an osculating circle with the centre lying on the axis l. The bisectors of the polygons $(r_{\bar{1}}, r, r_1)$ and $(r_{\bar{1}2}, r_2, r_{12})$ intersect at a point $c^{(2)}$ which lies on l. As in the continuous case for surfaces of revolution, $c^{(2)}$ may be identified as the centre of normal curvature associated with the edge (r, r_2). Indeed, the centre of the osculating circle is the image of the centre of normal curvature under normal projection as stated in a classical theorem by Meusnier [28]. Hence, if we denote the distance between r and $c^{(2)}$ by $\rho^{(2)}$, then it is natural to define the principal curvature associated with the discrete parallels by

$$\kappa^{(2)} = \frac{1}{\rho^{(2)}}. \tag{3.9}$$

An explicit expression for $\kappa^{(2)}$ is readily obtained if one introduces the decomposition

$$\Delta_2 r = \phi \bar{b}, \quad |\bar{b}| = 1 \tag{3.10}$$

and a 'discrete principal normal' n defined by

$$n = \frac{\Delta_{\bar{1}1} r}{|\Delta_{\bar{1}1} r|} = \frac{\Delta_{\bar{1}1} r}{2\sin(\gamma/2)} \tag{3.11}$$

Here, Δ_i and $\Delta_{\bar{i}i}$ constitute the forward first-order and central second-order difference operators, respectively, that is $\Delta_i f = f_i - f$, $\Delta_{\bar{i}i} f = f_{\bar{i}} - 2f + f_i$. Note that even though

(3.10) is reminiscent of (2.6b), the unit vectors $\boldsymbol{n}$ and $\bar{\boldsymbol{b}}$ are not orthogonal. Now, since γ does not depend on n_2, we obtain

$$\kappa^{(2)} = 2\frac{\bar{\boldsymbol{b}} \cdot \boldsymbol{n}}{\phi} = -\frac{\bar{\boldsymbol{b}} \cdot \Delta_2 \boldsymbol{n}}{\phi} \tag{3.12}$$

which is a natural discretization of (2.7b). Moreover, combination of relation (3.10) with its analogues corresponding to the vertices $\boldsymbol{r}_{\bar{1}}$ and $\boldsymbol{r}_{\bar{\bar{1}}}$, that is

$$\Delta_2 \boldsymbol{r}_{\bar{1}} = \phi_{\bar{1}} \bar{\boldsymbol{b}}_{\bar{1}}, \quad \Delta_2 \boldsymbol{r}_{\bar{\bar{1}}} = \phi_{\bar{\bar{1}}} \bar{\boldsymbol{b}}_{\bar{\bar{1}}} \tag{3.13}$$

with $\bar{\boldsymbol{b}}_{\bar{1}} = \bar{\boldsymbol{b}}_{\bar{\bar{1}}} = \bar{\boldsymbol{b}}$ produces

$$(\Delta_{\bar{\bar{1}}\bar{1}}\phi)\bar{\boldsymbol{b}} = \Delta_2 \Delta_{\bar{\bar{1}}\bar{1}} \boldsymbol{r} = \Delta_2[2\sin(\gamma/2)\boldsymbol{n}] = 2\sin(\gamma/2)\Delta_2 \boldsymbol{n} \tag{3.14}$$

by virtue of (3.11) and $\gamma_2 = \gamma$. Thus, multiplication by $\bar{\boldsymbol{b}}$ results in the standard discrete Schrödinger equation

$$\Delta_{\bar{\bar{1}}\bar{1}}\phi + \mathcal{K}\phi = 0 \tag{3.15}$$

if we set

$$\mathcal{K} = \kappa^{(1)}\kappa^{(2)} \tag{3.16}$$

as in the continuous case. It is therefore natural to regard (3.15) as the discrete Gauß equation for trapezoidal discrete surfaces.

To summarize, the fundamental relations (2.2), (2.4) and (2.7) have been discretized in a purely geometric manner. Their discrete counterparts are given by (3.15), (3.16) and (3.6), (3.12), respectively.

3.2. *Discrete surfaces of revolution*

As in the continuous case, trapezoidal discrete surfaces contain an important subclass of lattices which may be regarded as 'discrete surfaces of revolution'. Indeed, it is natural to consider a planar polygon $\Gamma: \boldsymbol{r} = \boldsymbol{r}(n_1)$ whose vertices are equidistant, that is $|\boldsymbol{r}_{\bar{1}} - \boldsymbol{r}| = 1$ without loss of generality (cf. Fig. 7). If we now successively rotate Γ around an axis which lies in the same plane by a finite angle $\omega = 2\pi/N$, $N \in \mathbb{N}$, then a discrete surface $\Sigma: \boldsymbol{r} = \boldsymbol{r}(n_1, n_2)$ is generated which possesses a $\mathbb{Z}_N$ rotational symmetry. It is evident that this discrete surface has the properties (i) and (ii) in the definition of trapezoidal quadrilateral lattices. The discrete meridians $n_2 = \text{const.}$ represented by Γ are the discrete geodesics while the discrete parallels $n_1 = \text{const.}$ consist of regular polygons ('discrete circles').

Without loss of generality, the position vector of discrete surfaces of revolution may be taken to be

$$\boldsymbol{r} = \begin{pmatrix} r(n_1)\cos(\omega n_2) \\ r(n_1)\sin(\omega n_2) \\ z(n_1) \end{pmatrix}, \tag{3.17}$$

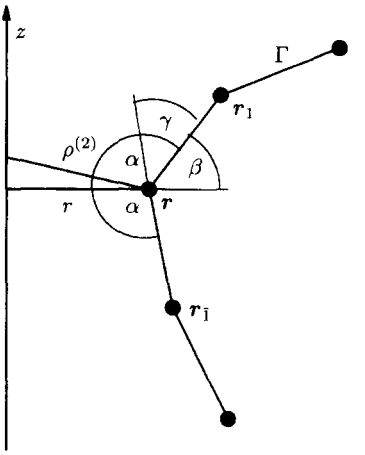

Fig. 7. The generator of a discrete surface of revolution.

where the functions $r(n_1)$ and $z(n_1)$ are related by the 'discrete arclength' condition

$$(\Delta_1 r)^2 + (\Delta_1 z)^2 = 1. \tag{3.18}$$

The latter may be solved identically by setting

$$\Delta_1 r = \cos\beta, \tag{3.19a}$$

$$\Delta_1 z = \sin\beta \tag{3.19b}$$

as indicated in Fig. 7. Consequently, the second radius of curvature at the vertex $\boldsymbol{r}$ reads

$$\rho^{(2)} = \frac{r}{\sin((\beta + \beta_{\bar{1}})/2)} \tag{3.20}$$

so that the principal curvatures become

$$\kappa^{(1)} = 2\sin\left(\frac{\beta - \beta_{\bar{1}}}{2}\right), \quad \kappa^{(2)} = \frac{\sin((\beta + \beta_{\bar{1}})/2)}{r}. \tag{3.21}$$

It is noted that the straight line l in Fig. 5 coincides with the axis of revolution in Fig. 7. Finally, combination of the relations (3.19a), (3.21) and application of a trigonometric identity produces

$$\Delta_{\bar{1}1} r + \mathcal{K} r = 0, \tag{3.22}$$

which is the discrete analogue of the Schrödinger equation (2.14). This result is in agreement with the fact that the decomposition (3.10) applied to the parametrization (3.17) leads to

$$\phi = 2r\sin\frac{\omega}{2} \tag{3.23}$$

and ϕ obeys the Schrödinger equation (3.15).

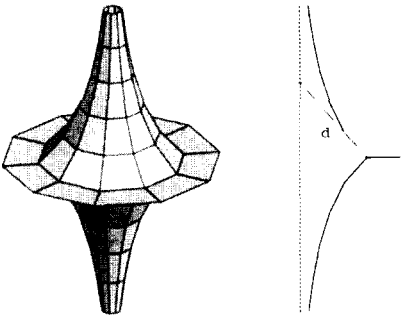

Fig. 8. The discrete tractrix as the generator of the discrete pseudosphere.

3.2.1. A discrete pseudosphere

As a first test of our definition of the discrete principal curvatures $\kappa^{(i)}$, we consider the case of constant discrete Gaußian curvature $\mathcal{K} = -\nu^2$. Since (3.22) now constitutes a linear difference equation with constant coefficients, it admits the first-order reduction

$$r_1 = \mu r, \tag{3.24}$$

where μ and $1/\mu$ are the roots of the characteristic equation $\mu^2 - (2 + \nu^2)\mu + 1 = 0$. If $\mu < 1$, then we denote by d the distance between the vertex $\boldsymbol{r}$ and the axis in the ('tangential') direction $\Delta_1 \boldsymbol{r}$ (cf. Fig. 8). Since $|\Delta_1 \boldsymbol{r}| = 1$, the relation

$$\frac{d-1}{d} = \frac{r_1}{r} = \mu \tag{3.25}$$

holds and hence d is constant as in the continuous case. For $\mu > 1$, a similar argument is applicable. We may therefore regard the polygon $\Gamma: \boldsymbol{r} = \boldsymbol{r}(n_1, 0)$ as a discrete tractrix which generates a discrete pseudosphere. Remarkably, in his book on difference geometry, Sauer [2] constructed the same discrete pseudosphere in a purely geometric manner by taking the condition $d = \text{const.}$ as a natural discretization of that defining the classical tractrix. The discrete pseudophere is displayed in Fig. 8.

3.2.2. A discrete Hasimoto surface of revolution

It is well known that the discrete Schrödinger equation (3.22) is form-invariant under a discrete version of the classical Darboux transformation [29]. In parallel with Section 2, we now investigate the action of a degenerate discrete Darboux transformation on (3.22). Thus, if r and $\hat{r}$ are two solutions of the discrete Schrödinger equation (3.22) with seed potential $\mathcal{K}$, then another solution of the discrete Schrödinger equation is given by

$$r' = \hat{r}_1 - \frac{r_1}{r}\hat{r}, \quad \mathcal{K}' - 2 = \frac{r^2}{r_1 r_{\bar{1}}}(\mathcal{K} - 2). \tag{3.26}$$

Once again, the Wronskian $w(r, \hat{r}) = r\hat{r}_1 - r_1\hat{r}$ is constant so that the above transformation reduces to

$$r' = \frac{c}{r}, \tag{3.27}$$

where c is an arbitrary constant.

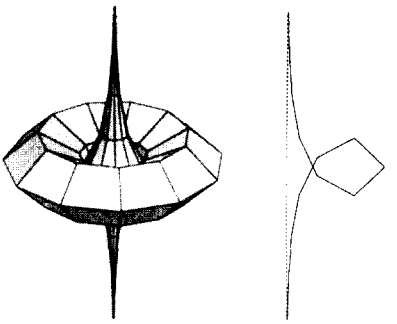

Fig. 9. A discrete Hasimoto surface of revolution and its generator.

As a seed potential, we now choose $\mathcal{K} = -\nu^2$ so that a particular solution of the discrete Schrödinger equation (3.22) is given by the 'discrete hyperbolic cosine':

$$r = \mu^{n_1} + \mu^{-n_1}. \tag{3.28}$$

It is readily shown that the new angle β' represents a discrete kink if the constant c in the transformation law (3.27) is chosen to be

$$c = 2\frac{\mu + 1}{\mu - 1}. \tag{3.29}$$

Indeed, for this value of c, the primed version of the relations (3.19a) and (3.19b) delivers

$$\beta' = 2\arctan\left(\frac{\mu^{n_1+1} - \mu^{-n_1}}{\mu + 1}\right) + \frac{\pi}{2} \tag{3.30}$$

and the new z-component of the position vector reads

$$z' = -n_1 + \left(\frac{\mu + 1}{\mu - 1}\right)\left(\frac{\mu^{n_1} - \mu^{-n_1}}{\mu^{n_1} + \mu^{-n_1}}\right). \tag{3.31}$$

The corresponding generator Γ' is depicted in Fig. 9. It contains a discrete loop and generates a discrete version of the Hasimoto surface of revolution displayed in Fig. 3.

The discrete Hasimoto surface of revolution as shown in Fig. 9 may be considered 'integrable' in the following sense. It is straightforward to show that

$$r' = \tilde{c}\tilde{\kappa}', \tag{3.32a}$$

$$\tilde{c} = \frac{1}{(\mu^{1/2} - \mu^{-1/2})^2}, \tag{3.32b}$$

$$\tilde{\kappa}' = 2\tan\left(\frac{\beta' - \beta'_{\bar{1}}}{2}\right). \tag{3.32c}$$

It is therefore natural to investigate the class of discrete surfaces of revolution defined by the relation

$$r = \tilde{c}\tilde{\kappa}, \quad \tilde{\kappa} = 2\tan\left(\frac{\beta - \beta_{\bar{1}}}{2}\right), \tag{3.33}$$

where $\tilde{c}$ is an arbitrary constant. In geometric terms, the quantity $\tilde{\kappa}$ is another measure for the curvature of the generator Γ. In fact, $1/\tilde{\kappa}$ is the radius of the dashed circle in Fig. 5 that touches two adjacent edges of Γ. It is noted that the centres of the 'osculating' circles associated with κ and $\tilde{\kappa}$ coincide. Now, insertion of the constraint (3.33) into (3.19a) results in the discrete pendulum equation

$$\tan\left(\frac{\beta_1-\beta}{2}\right)-\tan\left(\frac{\beta-\beta_{\bar{1}}}{2}\right)=\frac{1}{2\tilde{c}}\cos\beta. \tag{3.34}$$

Its kink solution is given by (3.30) if we parametrize $\tilde{c}$ according to (3.32c). Interestingly, the kink solutions (3.30) and

$$q=4\arctan\mu^{n_1} \tag{3.35}$$

of the standard integrable discrete pendulum equation [30]

$$\sin\left(\frac{q_1-2q+q_{\bar{1}}}{4}\right)=\left(\frac{\mu-1}{\mu+1}\right)^2\sin\left(\frac{q_1+2q+q_{\bar{1}}}{4}\right) \tag{3.36}$$

are related by

$$\beta'=\frac{q_1+q}{2}-\frac{\pi}{2}. \tag{3.37}$$

However, this connection between the discrete pendulum equations (3.34) and (3.36) is only valid in the case of the kink solutions. Thus, the constraint (3.37) leads to a *special* first integral which is common to both discrete pendulum equations. This particular integral of motion is then parametrized by the kink solution (3.30) (or (3.35)).

It turns out that the discrete pendulum equation (3.34) is indeed integrable. Thus, consider a polygon $\Gamma: \boldsymbol{r}=\boldsymbol{r}(n_1)$ with $|\Delta_1\boldsymbol{r}|=1$ so that

$$\boldsymbol{t}=\Delta_1\boldsymbol{r} \tag{3.38}$$

may be regarded as a discrete unit 'tangent'. It is then natural to interpret the unit vector which is perpendicular to the edges $\boldsymbol{t}$ and $\boldsymbol{t}_{\bar{1}}$, that is

$$\boldsymbol{b}=\frac{\boldsymbol{t}_{\bar{1}}\times\boldsymbol{t}}{|\boldsymbol{t}_{\bar{1}}\times\boldsymbol{t}|}=\frac{\boldsymbol{t}_{\bar{1}}\times\boldsymbol{t}}{\sin\gamma}=\cot\left(\frac{\gamma}{2}\right)\frac{\boldsymbol{t}_{\bar{1}}\times\boldsymbol{t}}{1+\boldsymbol{t}\cdot\boldsymbol{t}_{\bar{1}}}, \tag{3.39}$$

as the discrete binormal attached to the vertex $\boldsymbol{r}$, where γ is, as usual, defined by

$$\cos\gamma=\boldsymbol{t}\cdot\boldsymbol{t}_{\bar{1}}. \tag{3.40}$$

If we now assume in analogy with the Hasimoto vortex motion that the discrete curve Γ evolves in binormal direction with speed $\tilde{\kappa}$ in such a way that the 'discrete arclength condition' $|\Delta_1\boldsymbol{r}|=1$ is preserved, then compatibility of

$$\dot{\boldsymbol{r}}=\tilde{\kappa}\boldsymbol{b}=2\tan\left(\frac{\gamma}{2}\right)\boldsymbol{b} \tag{3.41}$$

and (3.38) produces the integrable differential–difference Heisenberg spin equation [17,18,27]

$$\dot{\boldsymbol{t}} = 2\Delta_1\left(\frac{\boldsymbol{t}_{\bar{1}} \times \boldsymbol{t}}{1 + \boldsymbol{t}\cdot\boldsymbol{t}_{\bar{1}}}\right). \tag{3.42}$$

Here, the overdot indicates differentiation with respect to time t.

Quispel et al. [19] have noted that the ansatz

$$\boldsymbol{t} = \begin{pmatrix} \cos\beta\cos 2\sigma t \\ \cos\beta\sin 2\sigma t \\ \sin\beta \end{pmatrix} \tag{3.43}$$

is admissible and reduces the differential–difference Heisenberg spin equation to a second-order difference equation for $x = \tan(\beta/2)$ which is contained in an 18-parameter class of integrable reversible mappings of the plane that may be parametrized in terms of elliptic functions. In the present context, the reduction (3.43) has a distinct geometric meaning. Indeed, the relation (3.38) shows that the position vector of Γ takes the form

$$\boldsymbol{r} = \begin{pmatrix} r(n_1)\cos 2\sigma t \\ r(n_1)\sin 2\sigma t \\ z(n_1) \end{pmatrix}, \tag{3.44}$$

where $r(n_1)$ and $z(n_1)$ are related to β by (3.19a) and (3.19b). Thus, the polygon Γ sweeps out a (semi-discrete) surface of revolution . Now, on the one hand, it is readily verified that

$$\dot{\boldsymbol{r}} = -2\sigma r\boldsymbol{b} \tag{3.45}$$

so that comparison with the evolution (3.41) reveals that the condition (3.33) is satisfied with $2\tilde{c}\sigma = -1$. On the other hand, the surface of revolution represented by (3.44) may be obtained from the discrete surfaces of revolution considered here in the limit $N \to \infty$. Hence, the constraint (3.43) reduces the differential–difference Heisenberg spin equation (3.42) to the discrete pendulum equation (3.34) since the latter does not depend on N. We therefore conclude that the class of discrete surfaces of revolution defined by (3.33) is governed by the integrable discrete pendulum equation (3.34).

3.2.3. Discrete Weingarten surfaces of revolution

In the preceding, we have made assumptions about the discrete Gaußian curvature $\mathcal{K} = \kappa^{(1)}\kappa^{(2)}$ in order to establish further analogies between the discrete and continuous cases. Here, as a first test of the appropriateness of the individual discrete principal curvatures $\kappa^{(1)}$ and $\kappa^{(2)}$, we consider the 'discrete Weingarten surfaces' of revolution defined by the relation

$$\kappa^{(1)} = c\kappa^{(2)}, \quad c = \text{const.} \tag{3.46}$$

Insertion of the definitions (3.21) into the above constraint and elimination of β by means of (3.19a) produces the second-order difference equation

$$\left(\frac{2r - c}{2r + c}\right)^2 = \left(\frac{1 + r_1 - r}{1 - r_1 + r}\right)\left(\frac{1 - r + r_{\bar{1}}}{1 + r - r_{\bar{1}}}\right). \tag{3.47}$$

Alternatively, elimination of r in favour of $x = \tan(\beta/2)$ leads to the second-order difference equation

$$\frac{2}{c}\left(\frac{1-x^2}{1+x^2}\right) = \frac{x_1+x}{x_1-x} - \frac{x+x_{\bar{1}}}{x-x_{\bar{1}}}. \tag{3.48}$$

Both equations may be brought into the compact form

$$X_1 = \frac{f^1(X) - X_{\bar{1}} f^2(X)}{f^2(X) - X_{\bar{1}} f^3(X)}. \tag{3.49}$$

The functions $f^i(X)$ may easily be calculated, depending on whether $X = r$ or $X = x$.

Within the class of difference equations (3.49), Quispel et al. [20] have isolated a 12-parameter subclass of equations which admit first integrals that are biquadratic and symmetric in X and X_1. Furthermore, these 'invariant curves' may be parametrized in terms of elliptic functions so that the corresponding two-dimensional mappings (3.49) are considered integrable. The 12-parameter class is given by

$$\boldsymbol{f}(X) = \begin{pmatrix} f^1(X) \\ f^2(X) \\ f^3(X) \end{pmatrix} = (A\boldsymbol{X}) \times (B\boldsymbol{X}), \quad \boldsymbol{X} = \begin{pmatrix} X^2 \\ X \\ 1 \end{pmatrix}, \tag{3.50}$$

where A and B are symmetric but otherwise arbitrary constant matrices, and the corresponding first integral reads

$$\frac{\boldsymbol{X}\cdot(A\boldsymbol{X}_1)}{\boldsymbol{X}\cdot(B\boldsymbol{X}_1)} = \text{const.} \tag{3.51}$$

In the case $c = 1$, that is $\kappa^{(1)} = \kappa^{(2)}$, the difference equation (3.47) is indeed a member of the above 12-parameter class. This does *not* apply to the difference equation (3.48). However, it is not difficult to show that the latter admits a first integral which turns out to be a discrete Riccati equation and hence may be linearized. In fact, it may be directly verified that

$$\beta = \gamma n_1 + \delta, \quad r = \frac{\sin(\beta-\gamma/2)}{2\sin(\gamma/2)}, \quad z = z_0 - \frac{\cos(\beta-\gamma/2)}{2\sin(\gamma/2)} \tag{3.52}$$

so that

$$\kappa^{(1)} = \kappa^{(2)} = \text{const.}, \quad r^2 + (z-z_0)^2 = \text{const.} \tag{3.53}$$

Accordingly, as in the continuous case, the principal curvatures are constant and the vertices of the discrete surface of revolution lie on a sphere.

The case of vanishing 'discrete mean curvature'

$$\mathcal{H} = \kappa^{(1)} + \kappa^{(2)} = 0, \tag{3.54}$$

that is $c = -1$, is of particular interest since the corresponding discrete surface of revolution may be interpreted as a 'discrete catenoid'. It turns out that neither the difference equation (3.47) nor (3.48), which may be written as

$$x^2 \Delta_{\bar{1}1} x = x_{\bar{1}} x_1 \Delta_{\bar{1}1} \frac{1}{x}, \tag{3.55}$$

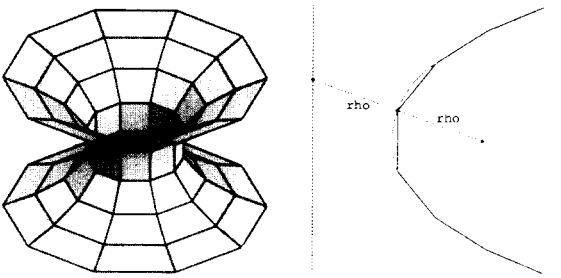

Fig. 10. The discrete catenoid and its generator.

may be located in the 12-parameter class. In fact, the functions f^i associated with (3.55) are given by (3.50) with

$$A = \begin{pmatrix} 0 & -1 & 0 \\ 2 & 0 & 2 \\ 0 & -1 & 0 \end{pmatrix}, \quad B = \begin{pmatrix} 0 & 0 & -1 \\ 0 & 2 & 0 \\ -1 & 0 & 0 \end{pmatrix}, \tag{3.56}$$

but the first integral (3.51) no longer holds since the matrix A is not symmetric. It is therefore desirable to classify the matrices A and B which allow integration of the mappings (3.49) and (3.50). Thus far, we have not been able to find non-trivial solutions to the difference equation (3.55).

The discrete catenoid along with its generator (discrete catenary) is displayed in Fig. 10. Note that, by construction, the distances from the vertex $\boldsymbol{r}$ to the centre of the corresponding osculating circle and the axis of revolution in 'normal' direction are the same. [2]

In the continuous setting, the case $c = 2$ turned out to be governed by the pendulum equation. Remarkably, in the discrete case, the functions $f^i(X = x)$ have the form (3.50) with *symmetric* matrices

$$A = \begin{pmatrix} 0 & 0 & 1 \\ 0 & -2 & 0 \\ 1 & 0 & 0 \end{pmatrix}, \quad B = \begin{pmatrix} 0 & 1 & 0 \\ 1 & 0 & 1 \\ 0 & 1 & 0 \end{pmatrix}. \tag{3.57}$$

Hence, the corresponding first integral reads

$$\tilde{K}(x - x_1)^2 = (x + x_1)(xx_1 + 1). \tag{3.58}$$

On the other hand, as pointed out in Section 3.2.2, the discrete pendulum equation (3.34) constitutes a symmetry reduction of the differential–difference Heisenberg spin equation with first integral [20]:

$$\begin{aligned}&(1 + 2K)x^2x_1^2 + \sigma(1 + K)(x^2x_1 + xx_1^2) + (1 + K)(x^2 + x_1^2) \\ &\quad +2Kxx_1 + \sigma(1 + K)(x + x_1) + 1 + 2K = 0,\end{aligned} \tag{3.59}$$

[2] It is evident that the trapezoidal quadrilateral lattices considered here are discrete isothermic in the sense of Bobenko and Pinkall [11] since the cross-ratio q of isosceles trapezoids is real. However, q depends on n_1 so that our discrete catenoid is different from that presented in [11].

where $x = \tan(\beta/2)$ and $2\tilde{c}\sigma = -1$. Comparison with (3.58) shows that the latter is a specialization ($K = -1/2$) of (3.59) if the identification $\tilde{K} = -1/\sigma$ is made. Thus, as in the continuous case, discrete Weingarten surfaces of revolution with $c = 2$ are contained in the 'discrete Hasimoto' class given by (3.33).

We conclude the paper with a curiosity. Let us regard the mapping (3.47) as a sequence $s_n = r(n)$ with initial data s_0 and s_1. If the constant c and s_0, s_1 are rational then the entire sequence s_n is rational by virtue of (3.49). Consequently, there exists integer-valued sequences p_n and q_n such that

$$\Delta s_n = \frac{p_n}{q_n}, \quad p_n, q_n \in \mathbb{Z}. \tag{3.60}$$

On the other hand, the mapping (3.47) may be brought into the form

$$[1 - (\Delta s_{n+1})^2] = \left(\frac{2s_{n+1} + c}{2s_{n+1} - c}\right)^2 \left(\frac{1 + \Delta s_{n+1}}{1 + \Delta s_n}\right)^2 [1 - (\Delta s_n)^2]. \tag{3.61}$$

If we now choose the initial data in such a way that $[1 - (\Delta s_0)^2]$ is a perfect square then $[1 - (\Delta s_n)^2]$ is a perfect square for all n, that is

$$[1 - (\Delta s_n)^2] = \frac{a_n^2}{b_n^2}, \quad a_n, b_n \in \mathbb{N}. \tag{3.62}$$

Hence, the latter and (3.60) imply that the sequence s_n generates suites of solutions of the Fermat equation

$$\bar{m}^2 + \bar{n}^2 = \bar{p}^2, \quad \bar{m}, \bar{n}, \bar{p} \in \mathbb{N}. \tag{3.63}$$

In geometric terms, this is reflected by the fact that the slope of the edges of the generator Γ is rational.

Acknowledgements

WKS would like to express his gratitude to the (visiting) members of the Dipartimento di Fisica, Università di Lecce for their hospitality.

References

[1] R. Sauer, Finite analoga zur differentialgeometrie der asymptotennetze, Ber. Math.-Tagung Tübingen (1946) 127–129.
[2] R. Sauer, Differenzengeometrie, Springer, Berlin, 1970.
[3] A. Bobenko, U. Pinkall, Discrete surfaces with constant negative Gaussian curvature and the Hirota equation, J. Differential Geom. 43 (1996) 527–611.
[4] A.I. Bobenko, W.K. Schief, Discrete indefinite affine spheres, in: A. Bobenko, R. Seiler (Eds.), Discrete Integrable Geometry and Physics, Oxford University Press, Oxford, to appear.
[5] A.I. Bobenko, W.K. Schief, Affine spheres: discretization via duality relations, J. Exp. Math., to appear.
[6] L.V. Bogdanov, B.G. Konopelchenko, Lattice and q-difference Darboux–Zakharov–Manakov systems via $\bar{\partial}$-dressing method, J. Phys. A 28 (1995) L173–L178.

[7] A. Doliwa, P.M. Santini, Multidimensional quadrilateral lattices are integrable, Phys. Lett. A 233 (1997) 365–372.
[8] W.K. Schief, Finite analogues of Egorov-type coordinates, Nonlinear Systems, Solitons and Geometry, Mathematisches Forschungsinstitut Oberwolfach, Germany, 1997 in preparation.
[9] R.R. Martin, J. de Pont, T.J. Sharrock, Cyclide surfaces in computer aided design, in: J.A. Gregory (Ed.), The Mathematics of Surfaces, Clarendon Press, Oxford, 1986, pp. 253–268.
[10] A.W. Nutbourne, The solution of the frame matching equation, in: J.A. Gregory (Ed.), The Mathematics of Surfaces, Clarendon Press, Oxford, 1986, pp. 233–252.
[11] A. Bobenko, U. Pinkall, Discrete isothermic surfaces, J. Reine Angew. Math. 475 (1996) 187–208.
[12] A. Bobenko, U. Pinkall, Discretization of surfaces and integrable systems, in: A. Bobenko, R. Seiler (Eds.), Discrete Integrable Geometry and Physics, Oxford University Press, Oxford, to appear.
[13] A. Bobenko, Discrete conformal maps and surfaces, in: P. Clarkson, F. Nijhoff (Eds.), Symmetries and Integrability of Difference Equations, London Mathematical Society, Lecture Note Series 255, Cambridge University Press, Cambridge, 1999, pp. 97–108.
[14] J. Cieśliński, A. Doliwa, P.M. Santini, The integrable discrete analogues of orthogonal coordinate systems are multidimensional circular lattices, Phys. Lett. A 235 (1997) 480–487.
[15] B.G. Konopelchenko, W.K. Schief, Three-dimensional integrable lattices in Euclidean spaces: conjugacy and orthogonality, Proc. R. Soc. London A 454 (1998) 3075–3104.
[16] C.F. Gauß, Disquisitiones Generales Circa Superficies Curvas, 1827; General Investigations on Curved Surfaces, Princeton, 1902.
[17] L.D. Faddeev, Lectures delivered at Les Houches Summer School, Preprint CEN-Saclay S. Ph.T./82/76.
[18] Y. Ishimori, An integrable classical spin chain, J. Phys. Soc. Jpn. 51 (1982) 3417–3418.
[19] G.R.W. Quispel, J.A.G. Roberts, C.J. Thompson, Integrable mappings and soliton equations, Phys. Lett. A 126 (1988) 419–421.
[20] G.R.W. Quispel, J.A.G. Roberts, C.J. Thompson, Integrable mappings and soliton equations II, Physica D 34 (1989) 183–192.
[21] L.P. Eisenhart, A Treatise on the Differential Geometry of curves and Surfaces, Dover, New York, 1960.
[22] G. Darboux, Comput. Rend. Acad. Sci. Paris 94 (1882) 1456–1459.
[23] H. Hasimoto, A soliton on a vortex filament, J. Fluid Mech. 51 (1977) 477–485.
[24] M. Lakshmanan, Continuum spin system as an exactly solvable dynamical system, Phys. Lett. A 61 (1977) 53–54.
[25] V.E. Zakharov, L.A. Takhtadzhyan, Equivalence of the nonlinear Schrödinger equation and the equation of a Heisenberg ferromagnet, Theoret. Math. Phys. 38 (1979) 17–23.
[26] A. Sym, Soliton surfaces VI. Gauge invariance and final formulation of the approach, Lett. Nuovo Cimento 41 (1984) 353–360.
[27] A. Doliwa, P. Santini, Geometry of discrete curves and lattices and integrable difference equations, in: A. Bobenko, R. Seiler (Eds.), Discrete Integrable Geometry and Physics, Oxford University Press, Oxford, to appear.
[28] K. Strubecker, Differentialgeometrie I, II, III, Sammlung Göschen, 1969.
[29] V.B. Matveev, M. Salle, Darboux transformations and solitons, Springer Series in Nonlinear Dynamics, Springer, Berlin, 1991.
[30] R. Hirota, Nonlinear partial difference equations. 3. Discrete sine-Gordon equation, J. Phys. Japan 43 (1977) 2079–2086.